PERGAMON

International Journal of Multiphase Flow 25 (1999) 1099–1128

International Journal of Multiphase Flow

www.elsevier.com/locate/ijmulflow

The local volumetric interfacial area transport equation: derivation and physical significance

Christophe Morel[a, 1], Nicolas Goreaud[a], Jean-Marc Delhaye[b,*]

[a]*CEA/Grenoble, DRN/DTP/SMTh/LMDS, 38054 Grenoble Cedex 9, France*
[b]*CEA/Grenoble, DRN/DTP, 38054 Grenoble Cedex 9, France*

Received 26 November 1998; received in revised form 30 April 1999

This paper is dedicated to Gad Hetsroni as a token of appreciation for the invaluable services he has offered to the multiphase flow community for so many years. 'Two are better than one' but there will be only one Gad Hetsroni for ever.

Abstract

In the two-fluid model, the closure relations for the mass, momentum and energy interfacial transfer terms involve the contact area between the phases per unit volume, namely the volumetric interfacial area. Ishii suggested that the local volumetric interfacial area should obey a transport equation. The main purpose of this paper is to derive this transport equation from geometrical considerations. No assumption on the interface configuration is needed so that the mathematical expression obtained for the transport velocity is valid for any two-phase flow regime. The physical significance of the transport velocity will be illustrated on some artificially generated bubbly flows with spherical bubbles. The link between the variables entering the transport equation and experimentally measurable quantities will be exemplified. The measurement of the local volumetric interfacial area and its transport velocity can be achieved by using four-sensor probes. As a preliminary study of real measurements, we have assessed the performance of some existing signal processing methods proposed for four-sensor probes on some artificially generated flows.

Keywords: Interfacial area; Transport equation; Four-sensor probe

* Corresponding author. Tel.: +33-4-7688-4275; fax: +33-4-7688-3196.
E-mail address: delhaye@dtp.cea.fr (J.M. Delhaye)
[1] Tel.: +33-4-7688-9227.

0301-9322/99/$ - see front matter
PII: S0301-9322(99)00040-3

1. Introduction

Among the different approaches used to model and simulate gas–liquid two-phase flows with or without phase change, the most general one is probably the two-fluid model since it describes each phase separately. In this model, a set of balance equations for mass, momentum and energy is written for each phase. The two phases are coupled through interfacial transfer terms for mass, momentum and energy which should verify the interfacial balance equations. These interfacial transfers generally depend upon the contact area between the phases per unit volume, namely the volumetric interfacial area. Thus, the determination of this volumetric interfacial area is of the utmost importance to correctly predict the evolution of two-phase flows by means of the two-fluid model.

Ishii (1975) suggested that the *local* volumetric interfacial area a_i should obey a transport equation having the following form:

$$\frac{\partial a_i}{\partial t_0} + \mathrm{div}(a_i \underline{V}_i) = \Phi_{a_i} \tag{1}$$

where $\underline{V}_i$ is the transport velocity of the volumetric interfacial area and Φ_{a_i} a source term taking into account the different phenomena creating or destroying interfacial area, such as coalescence or breakup of bubbles or droplets, phase change or interfacial stretching.

The first objective of this paper is to derive Eq. (1) without assuming any particular geometrical configuration of the interfaces, therefore, to prove that Eq. (1) can be applied independently of the flow regime. As a by-product of this derivation, the rigorous mathematical expression of the transport velocity $\underline{V}_i$ will be found. To begin with, the previous attempts to establish volumetric interfacial area transport equations similar to Eq. (1) by different authors will be discussed. The rigorous demonstration of Eq. (1) will then be given in Section 3. As the results obtained in Section 3 do not depend on the two-phase flow regime, we have chosen to illustrate our theory on the bubbly flow regime in Sections 4 and 5. Section 4 is devoted to the physical significance of Eq. (1), which will be shown not to be trivial, even for the simple case of a bubbly flow with spherical bubbles. Section 5 is devoted to the measurement of the local volumetric interfacial area and its transport velocity by means of a four-sensor probe. This type of probe has been chosen because their use is not limited to a particular two-phase flow regime. However, the accuracy of the measurement using a four-sensor probe depends on the size of the probe. We have thus simulated the behavior of such probes in an artificially generated bubbly flow with spherical bubbles in order to evaluate the effect of the finite size of the probe.

2. Previous derivations of the volumetric interfacial area transport equation

Achard (1978), Guido-Lavalle and Clausse (1991), Navarro-Valenti et al. (1991), Kocamustafaogullari and Ishii (1995) and Millies et al. (1996) gave a theoretical foundation for Eq. (1) by using a statistical formulation. These authors considered a *dispersed* flow and assumed that the particles constituting the dispersed phase (bubbles, droplets or solid particles)

could be characterized by some geometrical properties $\underline{\xi}$ such as a diameter, a shape factor.... The dispersed phase is then described in terms of a particle probability density function $f(\underline{\xi},\underline{x},t)$ defined in such a way that $f(\underline{\xi},\underline{x},t)|\mathrm{d}\underline{\xi}|\mathrm{d}V$ is the probable number of particles in the volume element $\mathrm{d}V$ around the point $\underline{x}$ having a vector of characteristic properties between $\underline{\xi}$ and $\underline{\xi}+\mathrm{d}\underline{\xi}$ at time t. The quantity $|\mathrm{d}\underline{\xi}|$ stands for $\mathrm{d}\xi_1\mathrm{d}\xi_2\ldots\mathrm{d}\xi_n$ so that $|\mathrm{d}\underline{\xi}|\mathrm{d}V=\mathrm{d}x_1\mathrm{d}x_2\mathrm{d}x_3\mathrm{d}\xi_1\mathrm{d}\xi_2\ldots\mathrm{d}\xi_n$ is the differential volume element in the phase space. This particle probability density function (pdf) must verify the Liouville-type equation (Hulburt and Katz, 1964; Tien and Lienhard, 1979):

$$\frac{\partial f}{\partial t}+\mathrm{div}\left[f\underline{c}\left(\underline{\xi},\underline{x},t\right)\right]+\sum_{j=1}^{n}\frac{\partial f\dot{\xi}_j}{\partial\xi_j}=h\left(\underline{\xi},\underline{x},t\right) \tag{2}$$

where n is the number of characteristic properties, $\underline{c}(\underline{\xi},\underline{x},t)$ the velocity of the center of a typical particle, $\dot{\xi}_j(\underline{\xi},\underline{x},t)$ the time rate of change of the jth characteristic property measured along the particle trajectory and $h(\underline{\xi},\underline{x},t)$ is a source term due to the coalescence/breakup and nucleation/collapse phenomena. In the statistical formulation, the volumetric interfacial area is defined as a particular statistical moment of the particle pdf:

$$a_{\mathrm{i}}(\underline{x},t)\hat{=}\int_{\Omega}A_{\mathrm{i}}\left(\underline{\xi}\right)f\left(\underline{\xi},\underline{x},t\right)|\mathrm{d}\underline{\xi}| \tag{3}$$

where $A_{\mathrm{i}}(\underline{\xi})$ is the interfacial area of a typical particle and Ω is the space of variation of the property vector $\underline{\xi}$. The volumetric interfacial area transport equation (1) can then be obtained by multiplying Eq. (2) by $A_{\mathrm{i}}(\underline{\xi})$ and integrating the resulting equation over Ω provided that:

$$\underline{V}_{\mathrm{i}}\hat{=}\frac{\displaystyle\int_{\Omega}A_{\mathrm{i}}\left(\underline{\xi}\right)\underline{c}\left(\underline{\xi},\underline{x},t\right)f\left(\underline{\xi},\underline{x},t\right)|\mathrm{d}\underline{\xi}|}{a_{\mathrm{i}}} \tag{4}$$

$$\Phi_{a_{\mathrm{i}}}\hat{=}\int_{\Omega}\left[A_{\mathrm{i}}\left(\underline{\xi}\right)h\left(\underline{\xi},\underline{x},t\right)+\sum_{j=1}^{n}\frac{\partial A_{\mathrm{i}}\left(\underline{\xi}\right)}{\partial\xi_j}\dot{\xi}_j f\left(\underline{\xi},\underline{x},t\right)\right]|\mathrm{d}\underline{\xi}| \tag{5}$$

It can be seen that the transport velocity defined by Eq. (4) corresponds to the *center of area velocity*. This result is valid for dispersed two-phase flows only and cannot be applied to other flow regimes with continuous interfaces like stratified or annular flows.

Candel and Poinsot (1990) derived a transport equation for the *volumetric flame area* in reacting single phase flows, a quantity analogous to the volumetric interfacial area in two-phase flows. The authors defined the volumetric flame area a_{i} as:

$$a_{\mathrm{i}}\hat{=}\frac{\mathrm{d}A}{\mathrm{d}V} \tag{6}$$

where $\mathrm{d}A$ is the elementary flame area embedded in an arbitrary unspecified volume element $\mathrm{d}V$. The authors then assume that $\mathrm{d}A$ and $\mathrm{d}V$ are convected by the same velocity $\underline{v}_{\mathrm{i}}$ and that this velocity is prescribed over the domain swept by the moving flame surface. Starting from

the Leibniz rule for the time rate of change of a volume integral, the authors have shown that:

$$\frac{1}{\mathrm{d}V}\frac{\mathrm{D_i d}V}{\mathrm{D}t} = \frac{1}{\mathrm{d}V}\left(\frac{\partial \mathrm{d}V}{\partial t} + \underline{v}_\mathrm{i}\cdot\underline{\nabla}\mathrm{d}V\right) = \mathrm{div}\ \underline{v}_\mathrm{i} \tag{7}$$

and starting from the corresponding rule for the time rate of change of a surface integral, they have shown that:

$$\frac{1}{\mathrm{d}A}\frac{\mathrm{D_i d}A}{\mathrm{D}t} = -\underline{n}_k\underline{n}_k{:}\underline{\underline{\nabla}}\underline{v}_\mathrm{i} + \mathrm{div}\ \underline{v}_\mathrm{i} \tag{8}$$

the right-hand side of Eq. (8) being the surface divergence of the velocity vector $\underline{v}_\mathrm{i}$.

If the flame front propagates in the normal direction at a speed S_L, the velocity $\underline{v}_\mathrm{i}$ will appear as the sum of the local fluid velocity $\underline{v}_\mathrm{k}$ and the flame speed in the normal direction (Candel and Poinsot, 1990):

$$\underline{v}_\mathrm{i} = \underline{v}_\mathrm{k} + S_\mathrm{L}\underline{n}_\mathrm{k} \tag{9}$$

Combining Eqs. (6)–(9), the authors obtained the following transport equation for a_i:

$$\frac{\partial a_\mathrm{i}}{\partial t} + \mathrm{div}\ a_\mathrm{i}\underline{v}_\mathrm{i} = -\left(\underline{n}_\mathrm{k}\underline{n}_\mathrm{k}{:}\underline{\underline{\nabla}}\underline{v}_\mathrm{k} - \mathrm{div}\ \underline{v}_\mathrm{k}\right)a_\mathrm{i} + a_\mathrm{i}S_\mathrm{L}\mathrm{div}\ \underline{n}_\mathrm{k} = a_\mathrm{i}\Phi_\mathrm{s} \tag{10}$$

where Φ_s is the source term of volumetric flame area per unit area. This source term comes from two main contributions: the effect of the fluid strain rate acting in the tangent plane and the effect of the flame curvature.

The method used by Candel and Poinsot (1990) is not satisfactory because the volumetric flame area Eq. (6) is not uniquely defined. Actually, it can be shown that, for a given area element $\mathrm{d}A$, the value of a_i depends on the choice of the volume element $\mathrm{d}V$ which surrounds $\mathrm{d}A$.

Coutris (1993) tried to establish the volumetric flame area transport equation by using the mass balance equation of a material surface $S(t)$ moving in space. If ρ_s represents the surface density, this balance equation can be written as:

$$\frac{\partial \rho_\mathrm{s}}{\partial t} + \mathrm{div_s}(\rho_\mathrm{s}\underline{v}_\mathrm{i}) = 0 \tag{11}$$

where $\underline{v}_\mathrm{i}$ is the velocity of a fixed point on surface $S(t)$ and $\mathrm{div_s}$ the surface divergence operator (Aris, 1962). By assuming that the volumetric flame area is defined as:

$$a_\mathrm{i} \hat{=} \frac{\rho_\mathrm{v}}{\rho_\mathrm{s}} \tag{12}$$

where ρ_v is the volumetric density of a membrane constituted by the surface $S(t)$ artificially thickened, and considering that the velocity $\underline{v}_\mathrm{i}$ is given by Eq. (9), Eq. (11) becomes:

$$\frac{\partial a_\mathrm{i}}{\partial t} + \mathrm{div_s}\left[a_\mathrm{i}\left(\underline{v}_\mathrm{k} + S_\mathrm{L}\underline{n}_\mathrm{k}\right)\right] + \frac{\partial a_\mathrm{i}S_\mathrm{L}}{\partial n} = a_\mathrm{i}\mathrm{div_s}\left(\underline{v}_\mathrm{k} + S_\mathrm{L}\underline{n}_\mathrm{k}\right) \tag{13}$$

an equation claimed by Coutris (1993) to be another form of Eq. (10). However, although the

volumetric flame area a_i is defined in a different way, it suffers from the same drawback as the one defined by Candel and Poinsot (1990) since thickening the interface is equivalent to choose a particular elementary volume.

Marle (1982) used the theory of distributions in order to derive the macroscopic equations governing multiphase flows in porous media. The volumetric interfacial area corresponding to the interface $\Sigma(t)$ between two phases or between one phase and the solid is defined by Marle (1982) as a convolution product:

$$a_i(\underline{x},t)\hat{=}(\delta_\Sigma * m)(\underline{x},t) = \int_{R^3} \delta_\Sigma(\underline{x}-\underline{y},t)m(\underline{y})\,\mathrm{d}\underline{y} = \int_{R^3} \delta_\Sigma(\underline{y},t)m(\underline{x}-\underline{y})\,\mathrm{d}\underline{y} \tag{14}$$

where δ_Σ is a Dirac distribution with the interface $\Sigma(t)$ as a support and $m(\underline{x})$ is a positive function with a compact support in R^3 given by the following relation:

$$m(\underline{x}) = \begin{cases} C\exp\left[-\left(r^2-|\underline{x}|^2\right)^{-1}\right] & \text{if } |\underline{x}|<r \\ 0 & \text{if } |\underline{x}|\geq r \end{cases} \tag{15}$$

the constant C being chosen in order to satisfy:

$$\int_{R^3} m(\underline{x})\,\mathrm{d}\underline{x} = 1 \tag{16}$$

The function $m(\underline{x})$ has been chosen of class C^∞ in order to ensure that any averaged quantity $f * m(\underline{x},t)$, such as the volumetric interfacial area given by Eq. (14), for example, will be also of class C^∞.

The volumetric interfacial area transport equation obtained by Marle (1982) reads:

$$\frac{\partial a_i}{\partial t} + \mathrm{div}\left[(\underline{v}_i\cdot\underline{n}_k)\underline{n}_k\delta_\Sigma * m\right] = -2H(\underline{v}_i\cdot\underline{n}_k)\delta_\Sigma * m + \sum(\underline{v}_L\cdot\underline{t}_L)\delta_L * m \tag{17}$$

where $\underline{v}_i$ and $\underline{n}_k$ are, respectively, the velocity vector and the unit normal vector defined on each point of the interface and H the mean curvature of the interface. The summation in the last term of Eq. (17) applies to the different contact lines $L(t)$ delimiting $\Sigma(t)$. The quantity δ_L is the Dirac distribution with support $L(t)$, $\underline{v}_L$ and $\underline{t}_L$ are, respectively, the velocity vector field of the boundary $L(t)$, and the unit vector tangent to the interface and normal to its boundary, outwardly directed.

Despite the fact that Eq. (17) does not involve any hypotheses, the different quantities it contains cannot be easily connected to experimentally measurable quantities.

Drew (1990) derived a volumetric interfacial area transport equation quite similar to that of Marle (1982). The volumetric interfacial area was defined by Drew (1990) as:

$$a_i(\underline{x},t)\hat{=}\left\langle\frac{\partial X_k}{\partial n}\right\rangle = \langle\underline{n}_k\cdot\underline{\nabla}X_k\rangle \tag{18}$$

where X_k is the characteristic function of phase 'k' and $\langle\,\rangle$ is an ensemble averaging operator. Note that the gradient of the characteristic function is non-zero only in the sense of distributions. The quantity $\underline{n}_k\cdot\underline{\nabla}X_k$ is a Dirac distribution with the different interfaces as a

support. The transport equation obtained by Drew (1990) reads:

$$\frac{\partial a_i}{\partial t} + \mathrm{div}(a_i \underline{V}_i) = -\bar{H}\frac{\partial \alpha_k}{\partial t} + \left\langle (H - \bar{H})(\underline{v}_i \cdot \underline{n}_k)\frac{\partial X_k}{\partial n} \right\rangle \tag{19}$$

where the transport velocity $\underline{V}_i$ and the mean curvature $\bar{H}$ are defined by the following relations:

$$\underline{V}_i \hat{=} \frac{\langle (\underline{v}_i \cdot \underline{n}_k)\underline{n}_k \partial X_k/\partial n \rangle}{a_i} \tag{20}$$

$$\bar{H} \hat{=} \frac{\langle H \partial X_k/\partial n \rangle}{a_i} \tag{21}$$

and the time fraction α_k is defined as the ensemble average of X_k. The first term in the right-hand side of Eq. (19) corresponds to the time rate of change of the volumetric interfacial area associated to the variation of the void fraction due to phase change and/or compressibility and dilatability of the phases. The second term in the right-hand side of Eq. (19) represents the rate of change of interfacial area due to bubble coalescence and breakup (Drew, 1990).

Eq. (19) suffers from the same drawbacks as Eq. (17) obtained by Marle (1982), i.e., the different quantities it contains cannot be easily connected to experimentally measurable quantities. However, the transport terms of Eqs. (17) and (19) both involve the speed of displacement $\underline{v}_i \cdot \underline{n}_k$ of the interfaces in the normal direction. The transport term we will obtain in Section 3 will also display the same characteristic feature.

The main objectives of the present paper are the following:

1. to derive a volumetric interfacial area transport equation valid for any flow configuration and free of any hypothesis,
2. to link the variables entering this transport equation to quantities which can be experimentally determined,
3. to explain the physical significance of the transport velocity entering the transport equation,
4. to assess the performance of some existing signal processing methods to be used with four-sensor probes.

3. Local volumetric interfacial area transport equation

3.1. Definitions and identities

A brief demonstration of the balance Eq. (1) is proposed in this section, a more detailed one being given by Morel (1997). The definitions of the volumetric interfacial areas as given by Delhaye (1976) are first recalled.

Let us first consider an arbitrary, fixed volume V (Fig. 1) which contains some interfaces having a total area $A_i(t)$. The instantaneous, *global* volumetric interfacial area is defined over

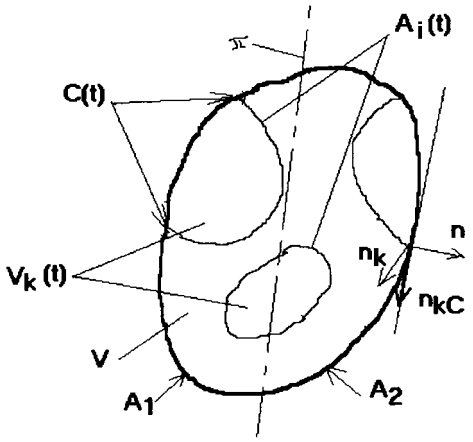

Fig. 1. Two-phase, fixed control volume.

the volume V by the following relation:

$$\Gamma(t)\hat{=}\frac{A_{\mathrm{i}}(t)}{V} \tag{22}$$

We then consider a given point (x,y,z) in volume V during a time interval $[T]$ centered on t_0. During this time interval, a finite number of interfaces pass through point (x,y,z), each interface having at point (x,y,z) a unit normal vector $\underline{n}_{\mathrm{k}}$ outwardly directed from phase 'k' and a displacement velocity $\underline{v}_{\mathrm{i}}\cdot\underline{n}_{\mathrm{k}}$, $\underline{v}_{\mathrm{i}}$ being the velocity of a fixed point on the interface. The *local* volumetric interfacial area is defined over the time interval $[T]$ by the following relation:

$$a_{\mathrm{i}}(x,y,z,t_0)\hat{=}\frac{1}{T}\sum_{J}\frac{1}{|\underline{v}_{\mathrm{i}}\cdot\underline{n}_{\mathrm{k}}|} \tag{23}$$

where the summation applies to all the interfaces J passing through (x,y,z) during $[T]$.

Delhaye (1976) proved the following identity, valid for any arbitrary vector field $\underline{B}_{\mathrm{k}}(\underline{x},t)$ associated with phase 'k':

$$\frac{1}{T}\int_{[T]}\frac{1}{V}\int_{A_{\mathrm{i}}(t)}\underline{B}_{\mathrm{k}}\cdot\underline{n}_{\mathrm{k}}\,\mathrm{d}a\,\mathrm{d}t\equiv\frac{1}{V}\int_{v}\frac{1}{T}\sum_{J}\frac{\underline{B}_{\mathrm{k}}\cdot\underline{n}_{\mathrm{k}}}{|\underline{v}_{\mathrm{i}}\cdot\underline{n}_{\mathrm{k}}|}\,\mathrm{d}v \tag{24}$$

where $\mathrm{d}a$ and $\mathrm{d}t$ are the area and time elements.

If the vector field $\underline{B}_{\mathrm{k}}$ is chosen such that $\underline{B}_{\mathrm{k}}\equiv\underline{n}_{\mathrm{k}}$ is verified on the interfaces, identity (24) becomes:

$$\frac{1}{T}\int_{[T]}\Gamma(t)\,\mathrm{d}t\equiv\frac{1}{V}\int_{v}a_{\mathrm{i}}(x,y,z,t_0)\,\mathrm{d}v \tag{25}$$

which is a fundamental identity connecting the two volumetric interfacial areas defined by Eqs. (22) and (23). For an arbitrary, fixed surface (S) intersecting the interfacial area $A_{\mathrm{i}}(t)$ through a curve $C(t)$, Eq. (24) results in the following equation (Delhaye and Achard, 1977):

$$\frac{1}{T}\int_{[T]}\int_{C(t)} \underline{B}_k \cdot \underline{n}_k \frac{dC}{\underline{n}_k \cdot \underline{n}_{kC}}\, dt \equiv \int_s \frac{1}{T}\sum_J \frac{\underline{B}_k \cdot \underline{n}_k}{|\underline{v}_i \cdot \underline{n}_k|}\, da \tag{26}$$

where $\underline{n}_{kC}$ is the unit normal vector to the curve $C(t)$ located in the tangential plane to the surface (S) at the point considered.

Definitions and identities Eqs. (22)–(26) will be used to derive Eq. (1). First, a balance equation for the global volumetric interfacial area $\Gamma(t)$ will be time-averaged over a time interval $[T]$, leading to Eq. (32) hereafter. Then, the local volumetric interfacial area transport Eq. (1) will be space-averaged over the volume V leading to Eq. (33) hereafter. The mathematical expressions of the transport velocity $\underline{V}_i$ and of the source term Φ_{a_i} will finally be obtained by identifying Eqs. (32) and (33).

3.2. The global volumetric interfacial area balance equation

The time rate of change of the interfacial area $A_i(t)$ contained in volume V at time t is equal to the flux of interfacial area through the boundary A of volume V, plus a production term per unit volume $\gamma(\underline{x},t)$:

$$\frac{dA_i(t)}{dt} = -\int_{C(t)} \mathrm{sgn}(\underline{n}_k \cdot \underline{n})(\underline{v}_i \cdot \underline{n}_k)\sqrt{1-(\underline{n}_k \cdot \underline{n}_{kC})^2}\frac{dC}{\underline{n}_k \cdot \underline{n}_{kC}} + \int_v \gamma(\underline{x},t)\, dv \tag{27}$$

where $\underline{n}$ is the unit vector normal to surface A and outwardly directed and $\underline{n}_{kC}$ the unit vector normal to the curve $C(t)$ located in the tangential plane to surface A, $C(t)$ being the intersecting curve between the two surfaces A and $A_i(t)$. The sign function 'sgn' is defined by:

$$\mathrm{sgn}(a) \hat{=} \frac{a}{|a|} \tag{28}$$

If surface A is subdivided into two complementary open surfaces A_1 and A_2 separated by an arbitrary plane π (Fig. 1), then the curve $C(t)$ is subdivided into two curves $C_1(t)$ and $C_2(t)$ located on the surfaces A_1 and A_2, respectively. Then, by splitting the first term in the right-hand side of Eq. (27) into two contributions and dividing by volume V, we obtain:

$$\begin{aligned}\frac{d\Gamma(t)}{dt} &+ \frac{1}{V}\int_{C_1(t)} \mathrm{sgn}(\underline{n}_k \cdot \underline{n}_1)(\underline{v}_i \cdot \underline{n}_k)\sqrt{1-(\underline{n}_k \cdot \underline{n}_{kC_1})^2}\frac{dC}{\underline{n}_k \cdot \underline{n}_{kC_1}} \\ &+ \frac{1}{V}\int_{C_2(t)} \mathrm{sgn}(\underline{n}_k \cdot \underline{n}_2)(\underline{v}_i \cdot \underline{n}_k)\sqrt{1-(\underline{n}_k \cdot \underline{n}_{kC_2})^2}\frac{dC}{\underline{n}_k \cdot \underline{n}_{kC_2}} = \frac{1}{V}\int_v \gamma(\underline{x},t)\, dv\end{aligned} \tag{29}$$

3.3. Time-averaging the global volumetric interfacial area balance equation

The balance Eq. (29) being an instantaneous one, it can be time-averaged over the time interval $[T]$:

$$\frac{1}{T}\int_{[T]} \frac{d\Gamma(t)}{dt}\, dt = \frac{\Gamma(t_0+T/2)-\Gamma(t_0-T/2)}{T} \cong \frac{d}{dt_0}\frac{1}{T}\int_{[T]} \Gamma(t)\, dt = \frac{d}{dt_0}\frac{1}{V}\int_v a_i\, dv =$$

$$\frac{1}{V}\int_v \frac{\partial a_i}{\partial t_0}\,\mathrm{d}v \tag{30}$$

where identity (25) and the fact that V is fixed have been used. Now, by using identity (26) with $S \equiv A_{1,2}$ and $\underline{B}_k \equiv \underline{v}_i \mathrm{sgn}(\underline{n}_k \cdot \underline{n}_{1,2})\sqrt{1-(\underline{n}_k \cdot \underline{n}_{kC_{1,2}})^2}$ we obtain:

$$\frac{1}{T}\int_{[T]}\int_{C_{1,2,(t)}} \mathrm{sgn}(\underline{n}_k \cdot \underline{n}_{1,2})(\underline{v}_i \cdot \underline{n}_k)\sqrt{1-(\underline{n}_k \cdot \underline{n}_{kC_{1,2}})^2}\frac{\mathrm{d}C}{\underline{n}_k \cdot \underline{n}_{kC_{1,2}}}\,\mathrm{d}t =$$

$$\int_{A_{1,2}} \frac{1}{T}\sum_J \frac{\mathrm{sgn}(\underline{n}_k \cdot \underline{n}_{1,2})(\underline{v}_i \cdot \underline{n}_k)\sqrt{1-(\underline{n}_k \cdot \underline{n}_{kC_{1,2}})^2}}{|\underline{v}_i \cdot \underline{n}_k|}\,\mathrm{d}a \tag{31}$$

By time-averaging Eq. (29) and using Eqs. (30) and (31), we obtain:

$$\frac{1}{V}\int_v \frac{\partial a_i}{\partial t_0}\,\mathrm{d}v + \frac{1}{V}\int_{A_1}\sum_J \frac{\mathrm{sgn}(\underline{n}_k \cdot \underline{n}_1)\mathrm{sgn}(\underline{v}_i \cdot \underline{n}_k)\sqrt{1-(\underline{n}_k \cdot \underline{n}_{kC_1})^2}}{T}\,\mathrm{d}a$$

$$+\frac{1}{V}\int_{A_2}\sum_J \frac{\mathrm{sgn}(\underline{n}_k \cdot \underline{n}_2)\mathrm{sgn}(\underline{v}_i \cdot \underline{n}_k)\sqrt{1-(\underline{n}_k \cdot \underline{n}_{kC_2})^2}}{T}\,\mathrm{d}a = \frac{1}{V}\int_v \frac{1}{T}\int_{[T]} \gamma(\underline{x},t)\,\mathrm{d}t\,\mathrm{d}v \tag{32}$$

3.4. Space averaging the local volumetric interfacial area transport equation

As the transport equation (1) proposed by Ishii (1975) is a local one, it can be space-averaged over volume V. By using the Gauss theorem, we get:

$$\frac{1}{V}\int_v \frac{\partial a_i}{\partial t_0}\,\mathrm{d}v + \frac{1}{V}\int_{A_1} a_i \underline{V}_i \cdot \underline{n}_1\,\mathrm{d}a + \frac{1}{V}\int_{A_2} a_i \underline{V}_i \cdot \underline{n}_2\,\mathrm{d}a = \frac{1}{V}\int_v \Phi_{a_i}\,\mathrm{d}v \tag{33}$$

The comparison of the Eqs. (32) and (33) leads to:

$$\int_{A_{1,2}}\sum_J \frac{\mathrm{sgn}(\underline{n}_k \cdot \underline{n}_{1,2})\mathrm{sgn}(\underline{v}_i \cdot \underline{n}_k)\sqrt{1-(\underline{n}_k \cdot \underline{n}_{kC_{1,2}})^2}}{T}\,\mathrm{d}a = \int_{A_{1,2}} a_i \underline{V}_i \cdot \underline{n}_{1,2}\,\mathrm{d}a$$

$$\int_v \left[\Phi_{a_i} - \frac{1}{T}\int_{[T]} \gamma\,\mathrm{d}t\right]\mathrm{d}v = 0 \tag{34}$$

The volume V and the surfaces A_1 and A_2 being arbitrary, we have:

$$\underline{V}_{\mathrm{i}} \cdot \underline{n} = \frac{\displaystyle\sum_{J} \frac{\mathrm{sgn}(\underline{n}_{\mathrm{k}} \cdot \underline{n})\mathrm{sgn}(\underline{v}_{\mathrm{i}} \cdot \underline{n}_{\mathrm{k}})\sqrt{1 - (\underline{n}_{\mathrm{k}} \cdot \underline{n}_{\mathrm{k}C})^2}}{T}}{\displaystyle\sum_{J} \frac{1}{T|\underline{v}_{\mathrm{i}} \cdot \underline{n}_{\mathrm{k}}|}} \tag{35a}$$

$$\Phi_{a_{\mathrm{i}}} = \frac{1}{T}\int_{[T]} \gamma \, \mathrm{d}t \tag{35b}$$

Therefore Eq. (1) which was proposed by Ishii (1975) is justified, provided that the transport velocity $\underline{V}_{\mathrm{i}}$ and the source term $\Phi_{a_{\mathrm{i}}}$ are expressed by the relations Eqs. (35a) and (35b), respectively, $\underline{n}$ defining an arbitrary oriented direction in space.

4. Application to bubbly flows

Although the results obtained in the preceeding section do not depend on the interfacial configuration, i.e., on the two-phase flow regime, we first investigate the simple case of bubbly flows with spherical bubbles to look for the physical significance of Eqs. (23) and (35a) which relate the volumetric interfacial area and its transport velocity to the speed of displacement and orientation of the interfaces.

One characteristic feature of the motion of a surface is that only the displacement velocity $\underline{v}_{\mathrm{i}} \cdot \underline{n}_{\mathrm{k}}$ can be uniquely defined. Expressions (23) and (35a) for the local volumetric interfacial area and its transport velocity both involve the displacement velocity of the interfaces $\underline{v}_{\mathrm{i}} \cdot \underline{n}_{\mathrm{k}}$, that is the velocity normal to the interface. This particular feature will have some consequences, which will be illustrated by the study of bubbly flows with spherical bubbles.

4.1. A single bubble moving vertically upwards

We first consider a single spherical bubble moving upwards along the z axis of a Cartesian reference frame. The bubble radius R and the bubble velocity U are assumed to be constant. At time $t = 0$, the center of the bubble is assumed to pass through the origin of the reference frame. Let us consider a fixed point (x,y,z) located on the trajectory of the bubble, and choose a time interval $[T]$ such that the interface of the bubble is passing through the point (x,y,z) at two times belonging to the time interval $[T]$. The calculation of the local volumetric interfacial area (23) and of its transport velocity (35a) gives:

$$a_{\mathrm{i}}(x,y) = \frac{2R}{UT\sqrt{R^2 - \left(x^2 + y^2\right)}} \tag{36}$$

$$\underline{V}_{\mathrm{i}}(x,y) = \begin{vmatrix} 0 \\ 0 \\ \dfrac{U}{R^2}\left[R^2 - \left(x^2 + y^2\right)\right] \end{vmatrix} \tag{37}$$

Since the bubble radius is constant, no interfacial stretching occurs and the source term Φ_{a_i} is nil:

$$\Phi_{a_i} = 0 \tag{38}$$

It is then easy to verify that the stationary form of the transport equation (1) is satisfied.

Eqs. (36) and (37) show that the volumetric interfacial area and its transport velocity only depend on the distance $r = \sqrt{x^2 + y^2}$ to the z axis. The profiles $a_i(r)$ and $V_{iz}(r)$ are presented in Fig. 2 for a bubble having a radius $R = 0.5$ and a velocity $U = 5$ (in arbitrary units).

It may seem quite surprising that the vertical component of the transport velocity V_{iz} is not equal to the bubble velocity U everywhere, according to the intuitive idea that the interface moves with the velocity of the bubble. In fact, this paradox can be raised by realizing that expressions (23) and (35a) involve the speed of displacement of the interface which is defined along the normal to the interface.

Let φ be the angle between the unit vector $\underline{n}_k$ normal to the bubble surface and the bubble velocity vector $\underline{U}$ (Fig. 3). Eqs. (36) and (37) now read:

$$a_i = \frac{2}{UT\cos\varphi} \tag{39}$$

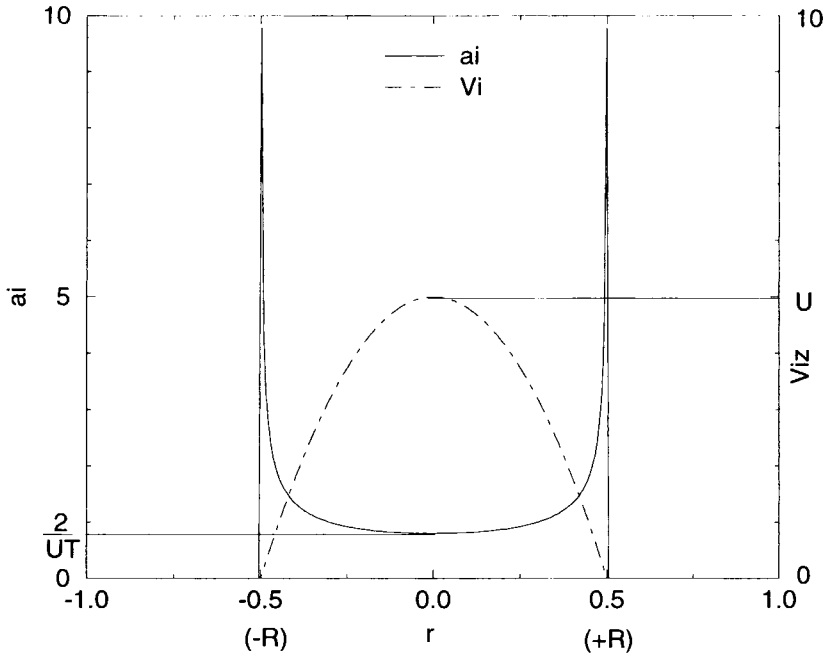

Fig. 2. Radial profiles $a_i(r)$ and $V_{iz}(r)$ for a spherical bubble moving vertically upwards (arbitrary units).

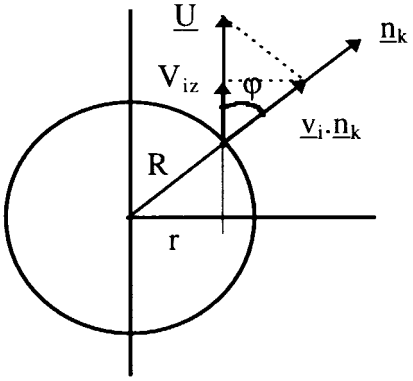

Fig. 3. Quantities characterizing a spherical bubble moving vertically upwards.

$$\underline{V}_{\mathrm{i}} = \begin{vmatrix} 0 \\ 0 \\ U\cos^2\varphi \end{vmatrix} \tag{40}$$

The z-component of the transport velocity $V_{\mathrm{i}z}$ averaged over the sphere is then equal to $U/3$.

The definition (23) of the local volumetric interfacial area involves the speed of displacement $\underline{v}_{\mathrm{i}} \cdot \underline{n}_{\mathrm{k}}$ of the interfaces passing through the considered point during the time interval $[T]$. It can be shown that this velocity corresponds to the scalar product of the bubble velocity $\underline{U}$ by the unit normal vector $\underline{n}_{\mathrm{k}}$. This explains the appearance of $\cos\varphi$ at the denominator of expression (39) for a_{i}. The vertical component of the transport velocity $V_{\mathrm{i}z}$ thus appears as the scalar product of the vector $(\underline{v}_{\mathrm{i}} \cdot \underline{n}_{\mathrm{k}})\underline{n}_{\mathrm{k}}$ and the unit vector $\underline{z}$ in the z direction.

We will now consider two more complex situations. The first one is a *steady bubbly flow* in a vertical duct with monodispersed spherical bubbles, where all bubbles move vertically upwards with the same velocity U, their initial position at the inlet of the duct being a random variable. The second situation is an *unsteady bubbly flow* with monodispersed spherical bubbles where a *bubble string* is progressing along the z axis of a vertical channel.

4.2. Simulation of a steady bubbly flow in a vertical duct

We have numerically calculated the radial profiles of the local volumetric interfacial area (23) and of its transport velocity (35a) in the case of N identical spherical bubbles of radius R moving vertically upwards with the same velocity $U\underline{z}$ in a vertical duct having a circular cross section of radius R_{c}. The initial position of each bubble in the inlet cross section of the duct $(x,y,0)$ is *randomly imposed*. The time interval $[T]$ is sufficiently large to have a large number N of bubbles passing through the measuring section during this time interval. The number N being large, one can expect that the bubble distribution in space is quite homogeneous.

Typical radial profiles $a_{\mathrm{i}}(r)$ and $V_{\mathrm{i}z}(r)$ are presented in Fig. 4 for bubbles of radius $R = 0.5$ rising with a velocity $U = 5$ in a pipe of radius $R_{\mathrm{c}} = 2$ (in arbitrary units).

In the core of the duct the profiles of a_{i} and $V_{\mathrm{i}z}$ are uniform. When one approaches the pipe wall a_{i} decreases linearly to zero and $V_{\mathrm{i}z}$ first increases up to a maximum located approximately at a distance to the wall equal to $3R/2$ and after decreases to zero. This wall

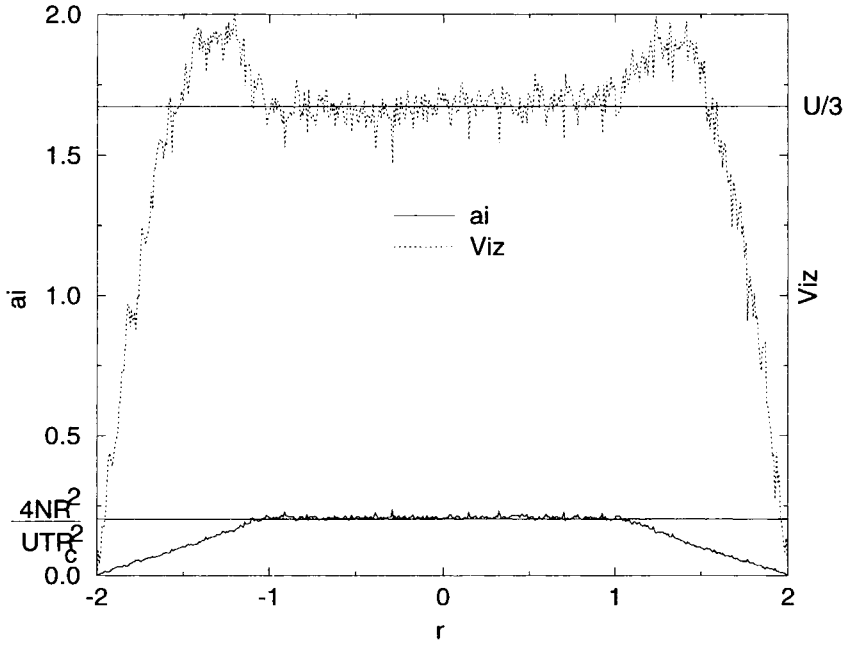

Fig. 4. Radial profiles $a_i(r)$ and $V_{iz}(r)$ for a stationary bubbly flow in a vertical duct with random initial positions of the bubbles (arbitrary units).

effect can be explained by the fact that a minimum distance between the center of each bubble and the wall, equal to the bubble radius R, is imposed when the initial position of the bubble is randomly generated. The uniform values of a_i and V_{iz} in the core can be determined analytically as it will be shown now.

The number of bubbles being large, the local volumetric interfacial area (23) can be approximated by the following statistical average:

$$a_i(x,y,z,t_0) = \frac{1}{S}\int\int_S p(r,\theta)a_{i,1B}(r,\theta)r\,dr\,d\theta \tag{41}$$

where S is the surface of the horizontal disk centered at point (x,y,z) and having a radius equal to the bubble radius R (Fig. 5), (r,θ) is the polar coordinate system describing the surface of the disk, $p(r,\theta)$ is the number of bubbles the center of which is passing through the point (r,θ) of the disk during $[T]$ and $a_{i,1B}(r,\theta)$ is the contribution to the local volumetric interfacial area calculated at point (x,y,z) of each bubble the center of which is passing through the point (r,θ). The contribution $a_{i,1B}(r,\theta)$ is given by Eq. (36).

The assumption of a homogeneous distribution of bubbles over the pipe cross section implies the following condition on $p(r,\theta)$:

$$\frac{1}{S}\int\int_S p(r,\theta)r\,dr\,d\theta = N\left(\frac{R}{R_c}\right)^2 \tag{42}$$

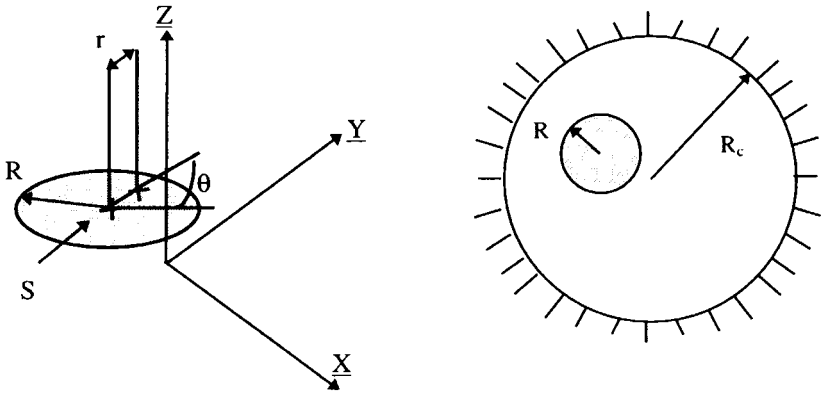

Fig. 5. Notations used for the determination of the local volumetric interfacial area.

If we consider that every point of the disk has the same probability to be crossed by the center of a bubble (this is true only if the distance between the center of the disk and the duct wall is equal to or greater than $2R$), then $p(r,\theta)$ is constant and the relation (42) gives:

$$p = N\left(\frac{R}{R_c}\right)^2 \tag{43}$$

Taking into account Eqs. (36) and (43), the local volumetric interfacial area given by Eq. (41) now reads:

$$a_i = \frac{4N}{UT}\left(\frac{R}{R_c}\right)^2 \tag{44}$$

Similarly, the core mean value of the vertical component of the transport velocity V_{iz} can be calculated by:

$$V_{iz} = \frac{\iint_S p(r,\theta)a_{i,1B}(r,\theta)V_{iz,1B}(r,\theta)r\,dr\,d\theta}{\iint_S p(r,\theta)a_{i,1B}(r,\theta)r\,dr\,d\theta} \tag{45}$$

where $V_{iz,1B}(r,\theta)$ is given by Eq. (37). The following simple result follows:

$$V_{iz} = \frac{U}{3} \tag{46}$$

which is consistent with the remark made about Eq. (40).

If the calculation point (x,y,z), namely the center of the disk S, is located at a distance to the wall less than $2R$, every point on the disk does not have the same probability to be crossed by the center of a bubble, this probability being even zero over a part of the disk. Consequently, expressions (44) and (46) are no longer valid. This explains the wall effect that can been observed on a_i and V_{iz} (Fig. 4) for distances to the wall less than one bubble diameter.

However, in the flow core the mean value of the transport velocity vertical component V_{iz} of the volumetric interfacial area for a swarm of bubbles randomly generated over the pipe cross section and moving upwards with the same rising velocity U, is only one third of this rising velocity.

This raises two important questions. The first question concerns the physical significance of the transport velocity appearing in Eq. (1): if the transport velocity $\underline{V}_i$ is generally smaller than the velocity of the bubbles, one could believe that the volumetric interfacial area associated to the bubbles will arrive at a given point *after* the bubbles. In fact, this is a false problem due to a misinterpretation of the transport Eq. (1). The following paragraph is devoted to the study of this problem by simulating and analyzing the propagation of a bubble string in a duct. The second question is the determination of a closure relation for the transport velocity $\underline{V}_i$. It constitutes the major issue for the introduction of a volumetric interfacial area transport equation in the two-fluid model. Only specific experiments will be capable of answering this question.

4.3. Simulation of the rise of a bubble string

In this section, we will study the rise of a bubble string along the axis of a vertical duct (Fig. 6). The bubbles are supposed to be spherical, monodispersed, regularly spaced, and moving with the same constant velocity U. In the case of a single bubble (Fig. 3), the transport velocity V_{iz} is given by Eq. (40) and is smaller than the bubble velocity U as long as the calculation point is not located on the z axis. The axial transport velocity being smaller than the bubble velocity, one could think that the volumetric interfacial area of the bubbles would strangely arrive at a given point *after* the bubbles. The study of the rise of a bubble string will show that this is a false problem due to a misinterpretation of the transport Eq. (1), and that this equation, after a proper space averaging, can be reduced to a kinematic wave propagation equation, the propagation velocity being equal to U.

Let us assume that initially the control volume does not contain any bubbles and that at

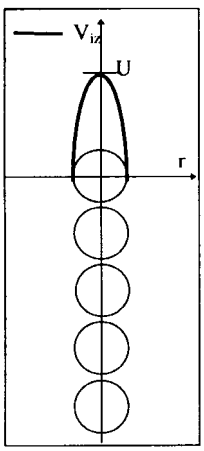

Fig. 6. Propagation of a bubble string.

time $t = 0$, the leading bubble of the bubble string passes through the inlet section of the control volume.

Fig. 7 shows the axial profiles $a_i(z)$ ansd $V_{iz}(z)$ calculated numerically at a given distance $r = 0.4$ from the z axis, for a bubble radius $R = 0.5$ and a bubble rising velocity $U = 5$ (arbitrary units). Three profiles $a_i(z)$ taken at three different times are compared in this figure. These profiles show that the propagation velocity of the volumetric interfacial area is equal to U (5 velocity units) whereas the value of V_{iz} is smaller than U (V_{iz} is approximately equal to 1.8 at the distance $r = 0.4$). In order to verify that the result illustrated in Fig. 7 is not contradictory with Eq. (1), we will evaluate the values of the different terms in this equation.

There is a difficulty to calculate the time and space derivatives of the volumetric interfacial area and of its transport velocity because these quantities are *piecewise continuous* functions as seen in Fig. 7. Therefore, it is necessary to space-average Eq. (1) in order to ensure the continuity of the quantities of interest. In our case, the source term Φ_{a_i} is zero because the bubbles have a constant radius and do not coalesce or breakup and the two velocity components V_{ix} and V_{iy} are nil:

$$\frac{\partial a_i}{\partial t_0} + \frac{\partial a_i V_{iz}}{\partial z} = 0 \tag{47}$$

Let us introduce the following space-averaging operator:

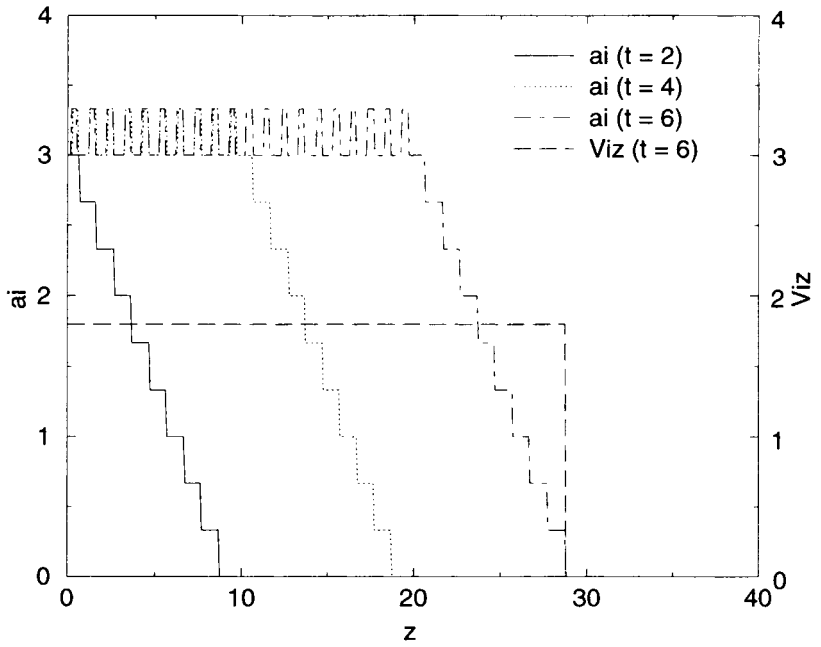

Fig. 7. Axial profiles of a_i and V_{iz} at a distance $r = 0.4$ to the axis (arbitrary units).

$$\bar{f}(x,y,z_0,t_0)\hat{=}\frac{1}{\Delta z}\int_{z_0-\frac{\Delta z}{2}}^{z_0+\frac{\Delta z}{2}} f(x,y,z,t_0)\,\mathrm{d}z \tag{48}$$

Commuting the space-averaging operator with the derivative operators can be achieved by using the limiting forms of the Leibniz rule and of the Gauss theorem applied to the segment $[\Delta z]$. If z_j $(j=1,\ldots,N_\mathrm{d})$ denotes the position of the jth discontinuity inside the segment $[\Delta z]$, N_d being the number of discontinuities situated in this space interval, the limiting forms of the Leibniz rule and of the Gauss theorem read:

$$\frac{\partial}{\partial z_0}\int_{[\Delta z]} f\,\mathrm{d}z=\int_{[\Delta z]}\frac{\partial f}{\partial z_0}\,\mathrm{d}z+\sum_{j=1}^{N_\mathrm{d}}\left[f\left(z_j^+\right)-f\left(z_j^-\right)\right]\quad z_j^\pm\hat{=}\lim_{\varepsilon\to 0}(z_j\pm\varepsilon) \tag{49}$$

$$\frac{\partial}{\partial t_0}\int_{[\Delta z]} f\,\mathrm{d}z=\int_{[\Delta z]}\frac{\partial f}{\partial t_0}\,\mathrm{d}z-U\sum_{j=1}^{N_\mathrm{d}}\left[f\left(z_j^+\right)-f\left(z_j^-\right)\right]\quad z_j^\pm\hat{=}\lim_{\varepsilon\to 0}(z_j\pm\varepsilon) \tag{50}$$

where we took into account the fact that all the discontinuities have the same velocity U.

By applying the averaging operator (48) to Eq. (47) and by using Eqs. (49) and (50), we obtain the following segment-averaged transport equation:

$$\frac{\partial \bar{a}_\mathrm{i}}{\partial t_0}+\frac{\partial\left(\overline{a_\mathrm{i}V_\mathrm{iz}}\right)}{\partial z_0}=\frac{1}{\Delta z}\sum_j\left[a_\mathrm{i}(V_\mathrm{iz}-U)|_{z_j^+}-a_\mathrm{i}(V_\mathrm{iz}-U)|_{z_j^-}\right] \tag{51}$$

We can then define the mean value of V_iz weighted by a_i:

$$\tilde{V}_\mathrm{iz}\hat{=}\frac{\overline{a_\mathrm{i}V_\mathrm{iz}}}{\bar{a}_\mathrm{i}} \tag{52}$$

Eq. (51) now reads:

$$\frac{\partial \bar{a}_\mathrm{i}}{\partial t_0}+\frac{\partial\left(\bar{a}_\mathrm{i}\tilde{V}_\mathrm{iz}\right)}{\partial z_0}=\frac{1}{\Delta z}\sum_j\left[a_\mathrm{i}(V_\mathrm{iz}-U)|_{z_j^+}-a_\mathrm{i}(V_\mathrm{iz}-U)|_{z_j^-}\right] \tag{53}$$

The axial profiles of the filtered variables $\bar{a}_\mathrm{i}$ and $\tilde{V}_\mathrm{iz}$ are represented in Fig. 8 for a length Δz of the segment $[\Delta z]$ containing 10 bubbles.

The numerical values of the two sides of Eq. (51) (or equivalently Eq. (53)) versus the axial distance z are given in Fig. 9. This figure shows that the two sides of Eq. (51) are nearly equal, the slight differences being due to the numerical errors when replacing the derivatives in the left-hand side of Eq. (51) by finite differences. We can therefore conclude that the volumetric interfacial area propagates with a velocity equal to the bubble velocity even if the transport velocity of its transport equation is smaller than the bubble velocity (Fig. 7) and this result is not contradictory with the transport Eq. (1) (Fig. 9).

Finally, we will demonstrate that, in the particular case considered here, Eq. (51) is equivalent to a kinematic wave propagation equation, with a propagation velocity equal to the

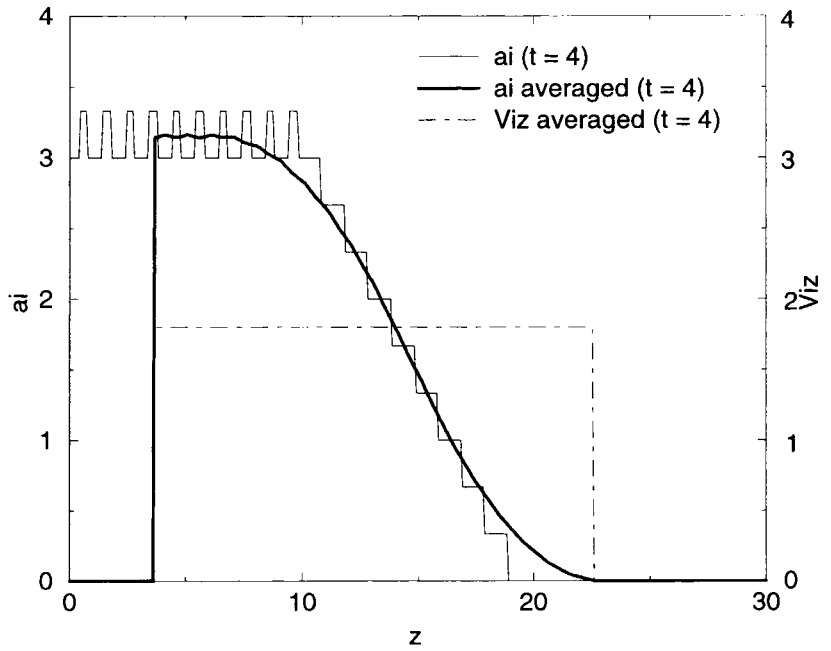

Fig. 8. Axial profiles of the filtered variables taken at time $t = 4$ (arbitrary units).

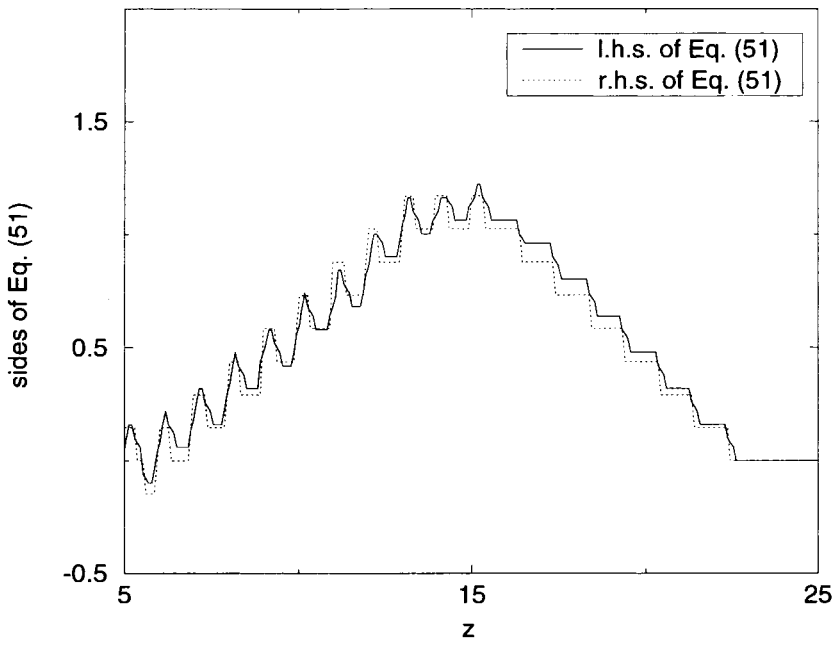

Fig. 9. Comparison of the two sides of Eq. (51) versus axial direction (arbitrary units).

bubble velocity. Eq. (51) can be rewritten as:

$$\frac{\partial \bar{a}_{\mathrm{i}}}{\partial t_0} + \frac{\partial \left(\overline{a_{\mathrm{i}} V_{\mathrm{iz}}}\right)}{\partial z_0} = \sum_j \frac{a_{\mathrm{i}} V_{\mathrm{iz}}\left(z_j^+\right) - a_{\mathrm{i}} V_{\mathrm{iz}}\left(z_j^-\right)}{\Delta z} - U \sum_j \frac{a_{\mathrm{i}}\left(z_j^+\right) - a_{\mathrm{i}}\left(z_j^-\right)}{\Delta z} \tag{54}$$

In the simple case considered here, the local volumetric interfacial area undergoes a jump at each discontinuity and is constant between two consecutive discontinuities (Fig. 7). Therefore, the sum of the jumps of a_{i} on all the discontinuities located within the segment $[\Delta z]$ is equal to the overall variation of a_{i} on this segment. The velocity V_{iz} being constant on the segment $[\Delta z]$ (Fig. 7), the same conclusion applies to the product $a_{\mathrm{i}} V_{\mathrm{iz}}$. We thus write:

$$\sum_j \frac{a_{\mathrm{i}}\left(z_j^+\right) - a_{\mathrm{i}}\left(z_j^-\right)}{\Delta z} = \frac{a_{\mathrm{i}}(z_0 + \Delta z/2) - a_{\mathrm{i}}(z_0 - \Delta z/2)}{\Delta z} \approx \frac{\partial \bar{a}_{\mathrm{i}}}{\partial z_0} \tag{55}$$

$$\sum_j \frac{a_{\mathrm{i}} V_{\mathrm{iz}}\left(z_j^+\right) - a_{\mathrm{i}} V_{\mathrm{iz}}\left(z_j^-\right)}{\Delta z} = \frac{a_{\mathrm{i}} V_{\mathrm{iz}}(z_0 + \Delta z/2) - a_{\mathrm{i}} V_{\mathrm{iz}}(z_0 - \Delta z/2)}{\Delta z} \approx \frac{\partial \overline{a_{\mathrm{i}} V_{\mathrm{iz}}}}{\partial z_0} \tag{56}$$

Accounting for Eqs. (55) and (56), Eq. (54) gives the following kinematic wave propagation equation:

$$\frac{\partial \bar{a}_{\mathrm{i}}}{\partial t_0} + U \frac{\partial \bar{a}_{\mathrm{i}}}{\partial z_0} = 0 \tag{57}$$

where the propagation velocity is equal to U.

This explains why the quantity a_{i} propagates with the velocity U although V_{iz} is smaller than U. However, this result cannot be generalized to more complex situations where the velocity U varies from one bubble to the other for example.

5. Application to the qualification of measuring techniques

This section is devoted to the measurement of the local volumetric interfacial area and its transport velocity by using four-sensor probes. The advantage of using four-sensor probes instead of two-sensor probes for the measurement of the volumetric interfacial area is that four-sensor probes can be used whatever the interfacial configuration, i.e., whatever the two-phase flow regime, as long as the interfaces have a finite speed of displacement.

The use of a four-sensor probe for interfacial area measurements was initiated by Kataoka and Serizawa (Kataoka et al., 1984, 1986, 1994).

For example, Revankar and Ishii (1993), Kojasoy et al. (1998) have used a four-sensor electrical resistivity probe to measure the local volumetric interfacial area, respectively, in a vertical air–water *cap bubbly flow* and in *horizontal slug flows*.

Although, in principle, the four-sensor probe method can be applied to all two-phase flow regimes, the accuracy of the measurement strongly depends on the ratio between the

characteristic size of the probe (the spacing distance between the sensors) and the local radius of curvature of the interfaces. Revankar and Ishii (1993) used a four-sensor probe with sensors spaced by a distance of 4 mm. Later Kim et al. (1998) used a modified four-sensor probe with sensors separated by 0.6 mm. Very recently, the Thermal-hydraulics and Physics Department of the Commissariat à l'Energie Atomique/Grenoble (France) has developed a four-sensor probe with typical spacing distances equal to 0.15 mm (Garnier, 1998).

The size and shape of the four-sensor probe certainly influence the interface motion. Therefore, it is obviously better to use small and well-designed probes to reduce the influence of the probe on the interfacial movements. A discussion on this problem can be found in Kim et al. (1998). Another problem related to the finite size of the probe is the possible occurrence of missing interfaces that do not touch each of the four sensors. The impact of this missing phenomenon on the measurements will be discussed in the following.

First, the theoretical foundation for the measurement of the local volumetric interfacial area established by Revankar and Ishii (1993) will be briefly recalled. We will then extend their theory to the measurement of the transport velocity $\underline{V}_i$ appearing in Eq. (1).

Finally, we will evaluate the uncertainty on the measurement of a_i and $\underline{V}_i$ due to the finite size of the probe on some numerically generated flows.

5.1. The four-sensor probe method

In this section, the method proposed by Revankar and Ishii (1993) to measure the local volumetric interfacial area a_i by means of a four-sensor probe is recalled and extended to the measurement of the transport velocity $\underline{V}_i$.

A four-sensor probe can be considered as a set of three double-sensor probes having a common sensor 0 (Fig. 10).

If x_0, y_0, z_0 denote the Cartesian coordinates of the sensor 0 in a given reference frame, the coordinates of the three other sensors 1, 2, 3 are given by the following relations:

$$\begin{aligned} x_k &= x_0 + \Delta s_k \cos(\eta_{xk}) \\ y_k &= y_0 + \Delta s_k \cos(\eta_{yk}) \quad (k = 1,2,3) \\ z_k &= z_0 + \Delta s_k \cos(\eta_{zk}) \end{aligned} \tag{58}$$

where Δs_k ($k = 1,2,3$) represents the distance between the sensor k and the sensor 0 (Fig. 10)

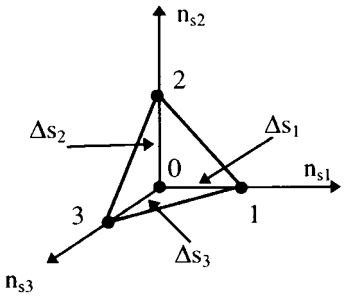

Fig. 10. Scheme of a four-sensor probe.

and $(\cos\eta_{xk}, \cos\eta_{yk}, \cos\eta_{zk})$ are the direction cosines of the unit vector $\underline{n}_{sk}$ $(k = 1,2,3)$ in the chosen reference frame.

Assuming that the jth interface, defined by the equation $F_j(x,y,z,t) = 0$, is passing through the four sensors at times t_j and $t_j + \Delta t_{kj}$ $(k = 1,2,3)$, we can write:

$$F_j(x_0,y_0,z_0,t_j) = 0 \tag{59}$$

$$F_j\left(x_k,y_k,z_k,t_j + \Delta t_{k_j}\right) = 0 \quad k = 1,2,3 \tag{60}$$

One can mesure the three flying times Δt_{kj} of the jth interface between sensors and define the following three velocities:

$$v_{sk_j} \hat{=} \frac{\Delta s_k}{\Delta t_{k_j}} \quad k = 1,2,3 \tag{61}$$

If the distances Δs_k $(k = 1,2,3)$ are sufficiently small in comparison to the radius of curvature of the jth interface, this interface is locally similar to a plane, and a first order Taylor expansion of the relations (60) near the point (x_0,y_0,z_0,t_j) gives the following set of equations:

$$\frac{\partial F_j}{\partial x}\cos\eta_{xk} + \frac{\partial F_j}{\partial y}\cos\eta_{yk} + \frac{\partial F_j}{\partial z}\cos\eta_{zk} = -\frac{\partial F_j}{\partial t}\frac{1}{v_{sk_j}} \quad k = 1,2,3 \tag{62}$$

Eq. (62) can then be solved for the three components of the vector $(\partial F_j/\partial x/\partial F_j/\partial t;$ $\partial F_j/\partial y/\partial F_j/\partial t;$ $\partial F_j/\partial z/\partial F_j/\partial t)$ if the probe geometry, defined by the nine direction cosines, and if the three velocities v_{sk_j} are known. As a result, the speed of displacement of the jth interface can be determined and the local volumetric interfacial area as well.

If the four sensors of the probe are arranged in an *orthogonal system*, the *local volumetric interfacial area* is obtained from the measured velocities v_{sk_j} by the following relation:

$$a_{\mathrm{i}} = \frac{1}{T}\sum_j \left\{ \left(\frac{1}{v_{s1_j}}\right)^2 + \left(\frac{1}{v_{s2_j}}\right)^2 + \left(\frac{1}{v_{s3_j}}\right)^2 \right\}^{1/2} \tag{63}$$

The above method, due to Revankar and Ishii (1993), assumes that the radius of curvature of an interface is much greater than the typical dimensions of the probe. When this is not the case, the second order terms of the Taylor expansion, not taken into account in Eq. (62), can be important. Moreover, some interfaces detected by the probe can miss one or several sensors. As indicated in Fig. 11, the orientation of such a missing interface in bubbly flow should be close to vertical orientation and therefore, its contribution to the local volumetric interfacial area must be substantial, as shown by the radial profile of a_{i} for a single bubble (Fig. 2).

Revankar and Ishii (1993) proposed to account for such missing interfaces in cap bubbly flows by imposing the following corrective value:

$$a_{\mathrm{i}} = \frac{\tau_{\mathrm{b}}}{T}\frac{l}{S} \tag{64}$$

where S is the projected area of the probe in the flow direction, l the distance between two

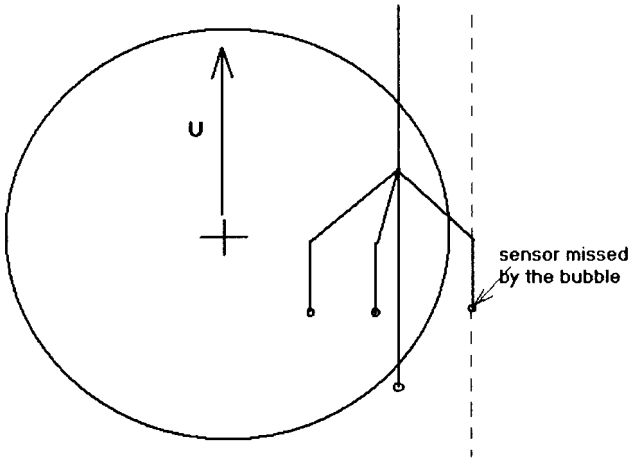

Fig. 11. Missing signal.

downstream sensors and τ_b the residence time of the bubble on the detecting sensor. However, the physical significance of expression (64) should still be firmly substantiated.

The method proposed by Revankar and Ishii (1993) can be extended to the measurement of the transport velocity $\underline{V}_i$. Eq. (35a) can be rewritten as:

$$a_i \underline{V}_i \cdot \underline{n} = \frac{1}{T} \sum_j \mathrm{sgn}(\underline{v}_i \cdot \underline{n}_k)\mathrm{sgn}(\underline{n}_k \cdot \underline{n})\sqrt{1 - (\underline{n}_k \cdot \underline{n}_{kC})^2} \tag{65}$$

where $\underline{n}$ is an arbitrary direction in space.

The right-hand side of Eq. (65) involves, for each interface, the unit normal vectors $\underline{n}_k$ and $\underline{n}_{kC}$ in addition to the interfacial displacement velocity $\underline{v}_i \cdot \underline{n}_k$ (Fig. 1). The unit vector normal to the jth interface is defined by the relation:

$$\underline{n}_{k_j} \hat{=} \frac{\underline{\nabla} F_j}{|\underline{\nabla} F_j|} \tag{66}$$

This vector can be obtained from the resolution of the system of equations (62). The vector $\underline{n}_{kC}$ is then determined by projecting the vector $\underline{n}_k$ on the plane normal to the $\underline{n}$ direction, and by making its modulus equal to one.

For the interfaces missing one or several sensors of the four-sensor probe, no corrective value is proposed for $\underline{V}_i$ since such missing interfaces are nearly vertical (Fig. 11) so that the transport velocity V_{iz} tends to zero (Fig. 2).

5.2. Simulations of the response of a four-sensor probe in bubbly flow

The behavior of a four-sensor probe in an artificially generated bubbly flow with spherical bubbles has been numerically simulated. The objective was to evaluate the uncertainty in the measurement of a_i and $\underline{V}_i$ due to the finite size of the probe. This uncertainty can be

determined by comparing the values of a_i and $\underline{V}_i$ obtained from the probe signals with their *exact* values calculated from the equations of the different interfaces.

The flow considered in this section is a bubbly flow in a vertical duct of circular cross section, the radius of the duct R_c being equal to 0.1 m. A number of 10,000 bubbles move vertically upwards through the measuring section for each run, their initial positions in the inlet cross section $(x,y,0)$ being *randomly imposed* (as in Section 4.2). The bubbles are spherical, monodispersed, and have a constant radius $R = 15$ mm and a constant rising velocity $U = 0.2$ m/s. The dimension of the probe $\Delta s_1 = \Delta s_2 = \Delta s_3 = \Delta s$ was varied from one run to another one in order to investigate the influence of the size ratio $\Delta s/R$ on the accuracy of the measurement.

The comparison between the simulated profiles $a_i(r)$ and $V_{iz}(r)$ obtained from the probe signals and the exact profiles are presented in Figs. 12 and 13 for four different values of the

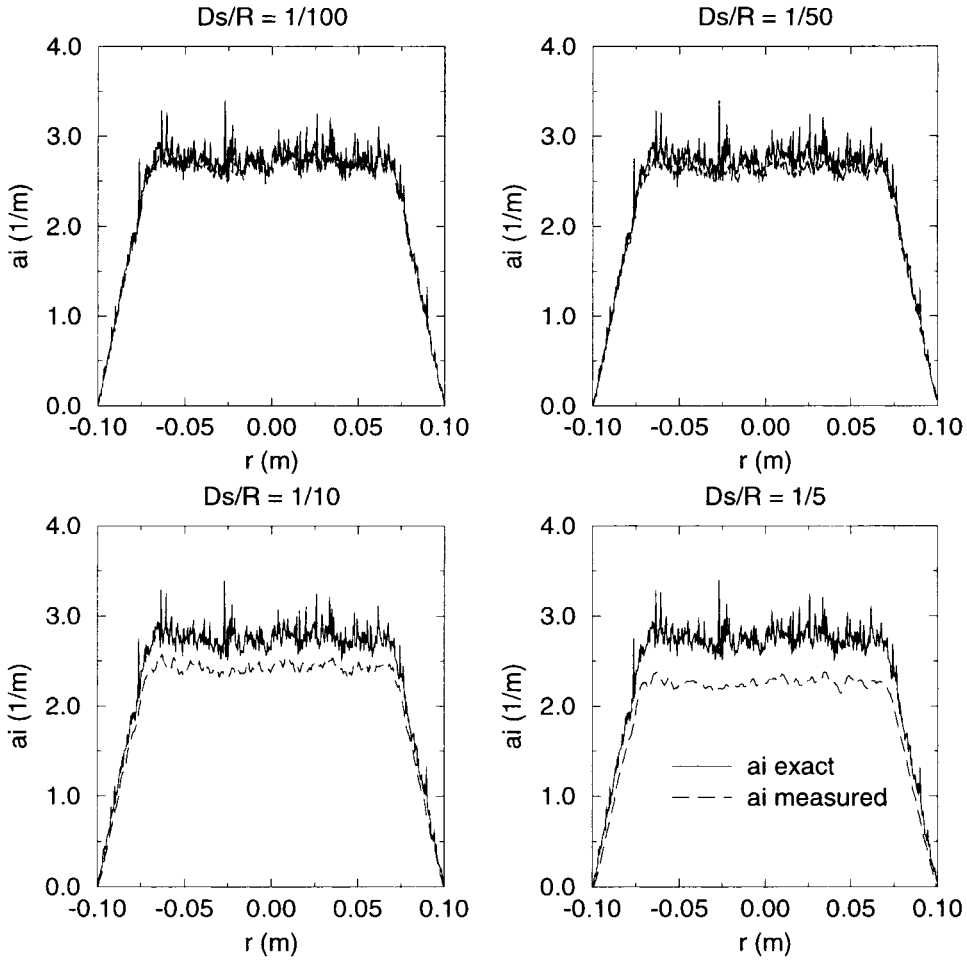

Fig. 12. Comparison between the simulated profiles $a_i(r)$ determined from probe measurements and the exact profiles for different values of the size ratio $\Delta s/R$.

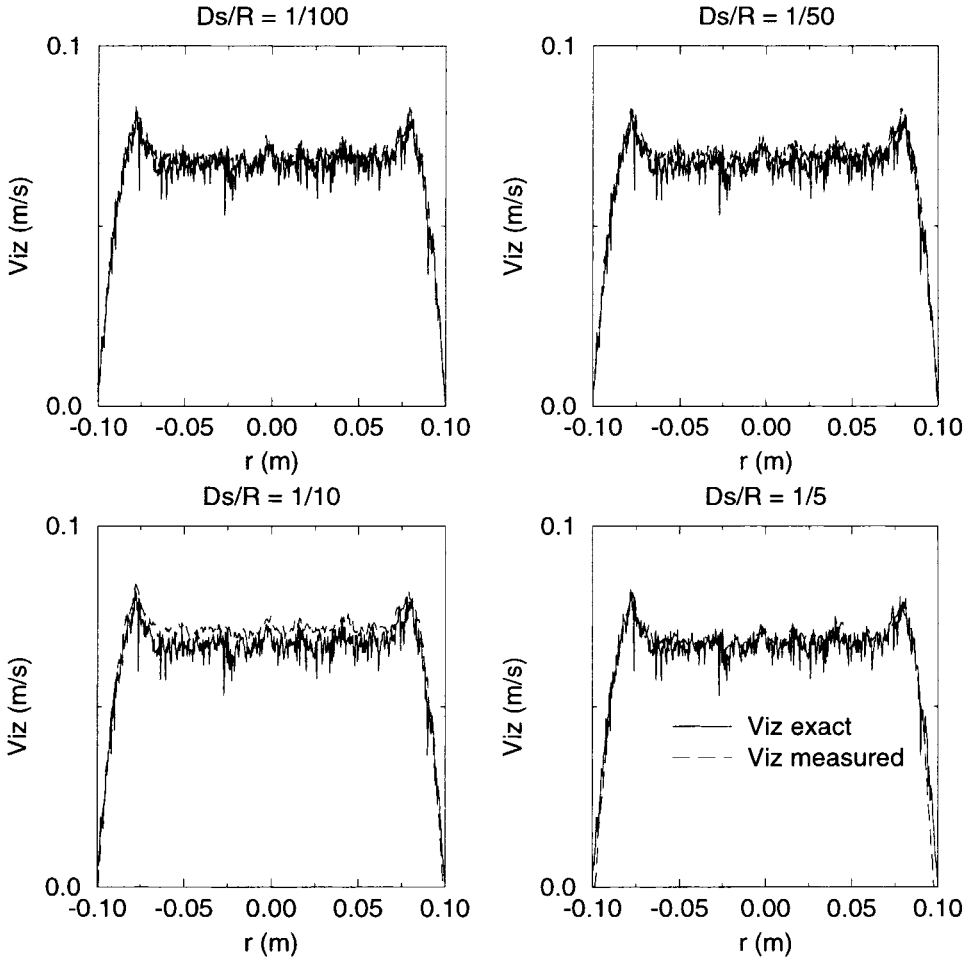

Fig. 13. Comparison between the simulated profiles $V_{iz}(r)$ determined from probe measurements and the exact profiles for different values of the size ratio $\Delta s/R$.

ratio $\Delta s/R$. In the determination of the simulated radial profile of a_i, the interfaces which have missed one or several sensors of the probe have been taken into account using the corrective value (64) proposed by Revankar and Ishii (1993). No corrective value was used for V_{iz} as suggested above.

Fig. 12 shows that, when the ratio $\Delta s/R$ is equal to 1/100 or 1/50, the measured and exact profiles of the local volumetric interfacial area are very close together, the measured one being smoother. For higher values of the ratio $\Delta s/R$, the four-sensor probe under-estimates the local volumetric interfacial area up to 20% for a ratio $\Delta s/R$ equal to 1/5.

Fig. 13 shows that the error on the measurement of V_{iz} is smaller than the error on the measurement of a_i. Moreover, this error over-estimates the value of V_{iz}, and does not

significantly increase with the size of the probe (the biggest differences observed between the measured V_{iz} and the exact one concern the run with $\Delta s/R = 1/10$).

It is not surprising that the uncertainty on the measurement of V_{iz} does not increase with the size of the probe as for the measurement of a_i. This error comes essentially from the interfaces that miss one or several sensors of the probe. As it was shown in the preceding section, such missing interfaces are nearly vertical (Fig. 11), therefore, bringing a major contribution to the volumetric interfacial area but a minor contribution to the transport velocity, as it can be seen on a single bubble (Fig. 2).

5.3. Simulation of the response of a four-sensor probe in a polydispersed bubbly flow with spherical bubbles

In real flows, the bubbles are not monodispersed and their size can vary over one order of magnitude. When the bubbles are polydispersed, the size ratio $\Delta s/R$ varies from one bubble to the other. The smaller the bubbles, the greater the probability to miss one or several sensors of the probe and to give erroneous value of the interfacial area, as it has been shown in the preceding section. In real slug flows, for example, the large gas plugs are generally much less numerous than the small spherical bubbles that are continuously entrained in their wakes. In such a situation, the large gas plugs contain the essential part of the void fraction, but the essential part of the interfacial area comes from the much more numerous small spherical bubbles.

A simulation was performed to investigate the capability of a four-sensor probe to measure the local volumetric interfacial area and its transport velocity in a *polydispersed* bubbly flow. The bubbles were spherical, but their size, as well as their initial position, were randomly imposed. The size of the bubbles was varied between Δs and $100\Delta s$, giving a ratio $\Delta s/R$ varying between 1/100 and 1. The results of this simulation are presented in Fig. 14.

Fig. 14 shows a very good agreement between the exact and measured quantities for a polydispersed bubbly flow. However, this result is somewhat artificial because in real flows, the size distribution of the bubbles is generally not uniform as in our simulation, but is characterized by the existence of several peaks. For example, in slug flows, there are generally two distinct peaks associated with the gas plugs and the small spherical bubbles respectively.

Another simulation (Fig. 15) was made with the bubble radius varying from $0.1\Delta s$ to $10\Delta s$. Almost 10% of the bubbles were smaller than the spacing distance between the sensors of the probe Δs and 20% were smaller than $2\Delta s$. As for the cases with monodispersed bubbles and values of Δs not negligible in comparison to the bubble radius R, the local volumetric interfacial area is under-estimated, unlike the transport velocity that is well reproduced by the probe measurement. In fact, it is not surprising that the velocity is well reproduced without a corrective value for missing interfaces, because the contributions of the different bubbles are cumulative on the volumetric interfacial area, but not on the transport velocity.

In the last simulation (Fig. 16), the bubble radius was varied from $0.1\Delta s$ to $5\Delta s$, therefore, almost 20% of the bubbles were smaller than Δs and 40% smaller than $2\Delta s$. In this case, even the transport velocity was under-estimated by the probe measurement.

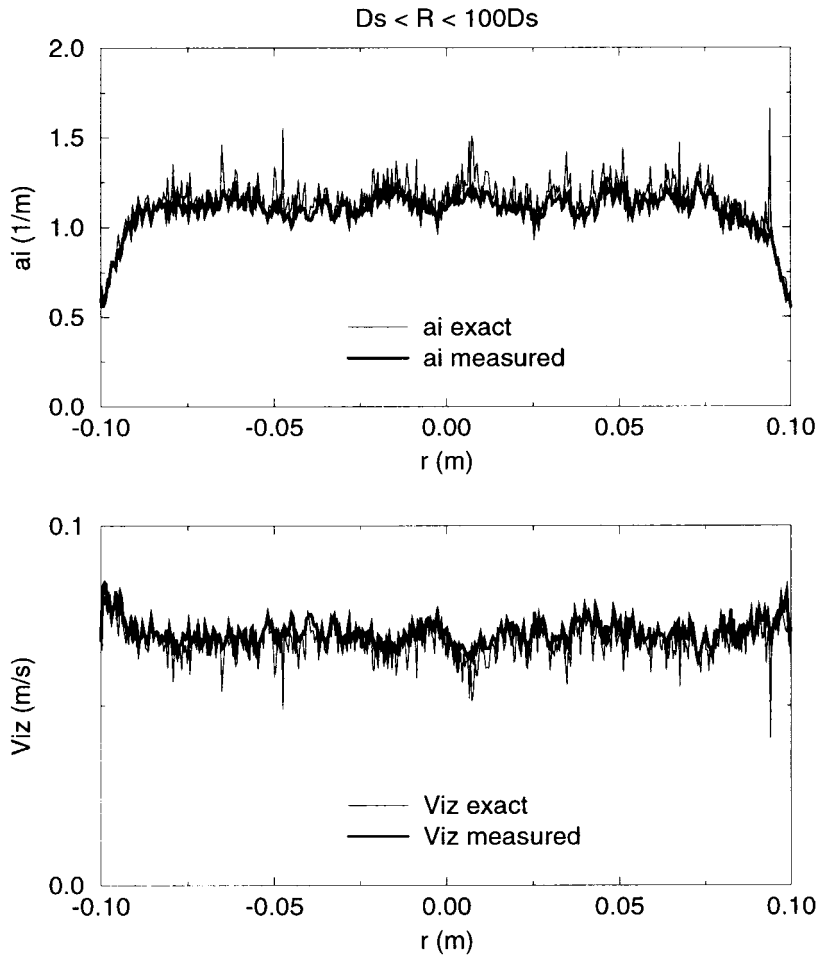

Fig. 14. Comparison between the measured and exact profiles $a_i(r)$ and $V_{iz}(r)$ in a polydispersed bubbly flow with spherical bubbles ($\Delta s < R < 100\Delta s$).

6. Conclusion

The local volumetric interfacial area transport Eq. (1) proposed by Ishii (1975) was derived by using geometrical considerations which do not require any assumptions on the interfacial configuration, i.e., on the two-phase flow regime. The mathematical expression of the transport velocity appearing in Eq. (1) is given by the relation (35a).

These results were applied to a bubbly flow with spherical bubbles. Several issues have been raised, the first one being the fact that the transport velocity of the interfacial area in bubbly flows is generally smaller than the bubble velocity. It was explained that the local volumetric interfacial area a_i, defined by Eq. (23), and its transport velocity $\underline{V}_i$, defined by Eq. (35a), both involve the speed of displacement of the interfaces which is a velocity normal to the interfaces. As a consequence it was shown that in the steady flow of a swarm of spherical bubbles moving

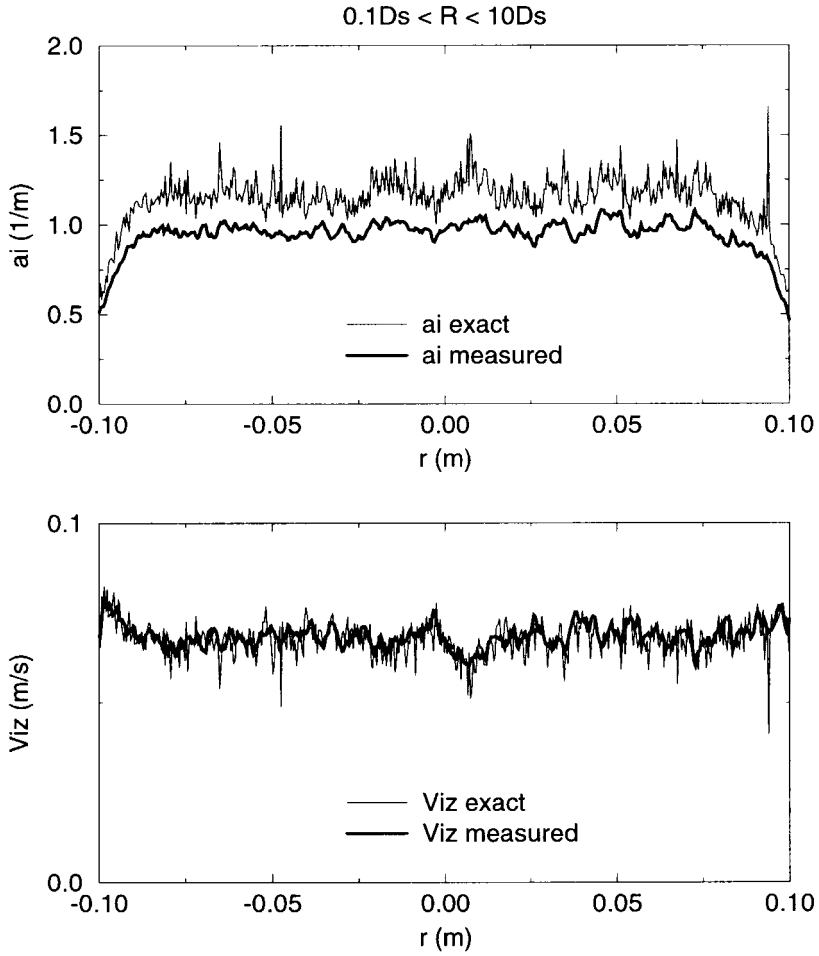

Fig. 15. Comparison between the measured and exact profiles $a_i(r)$ and $V_{iz}(r)$ in a polydispersed bubbly flow with spherical bubbles ($0.1\Delta s < R < 10\Delta s$).

upwards with the same velocity $\underline{U}$, the transport velocity $\underline{V}_i$ is only one third of the bubble velocity. The study of a bubble string propagation has also shown that the spatial variations of a_i propagate at the same velocity than the bubbles, although the transport velocity is less than the bubble string velocity. It was shown that this result was not contradictory with Eq. (1) and that this equation could be reduced to a kinematic wave propagation equation after a proper spatial averaging, the propagation velocity being equal to the bubble velocity.

Our method can be compared to the other methods found in the literature. The transport terms of Eq. (17) established by Marle (1982) and (19) established by Drew (1990) also involve the speed of displacement $\underline{v}_i \cdot \underline{n}_k$ normal to the interfaces. The methods used by these authors, involving the concept of distributions, is quite analogous to the method we have developed here, even if the obtained equations are different in their mathematical form. The method based on a statistical formulation Eqs. (2)–(5), applicable to dispersed flow regimes, does not lead to a transport velocity smaller than the bubble velocity. Actually, it can be easily seen

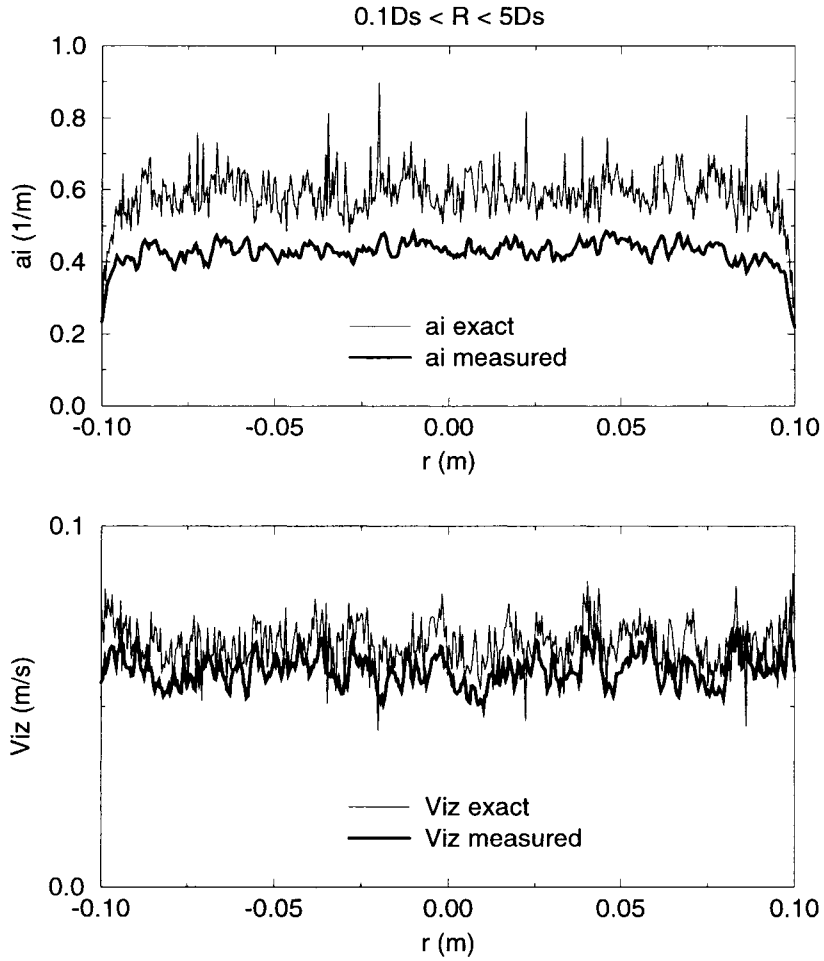

Fig. 16. Comparison between the measured and exact profiles $a_i(r)$ and $V_{iz}(r)$ in a polydispersed bubbly flow with spherical bubbles ($0.1\Delta s<R<5\Delta s$).

from Eq. (4) that the transport velocity $\underline{V}_i$ is equal to the bubble velocity, denoted in this equation by $\underline{c}$, as soon as this bubble velocity does not depend on the bubble considered. However, it must be noted that the statistical method is based on a definition Eq. (3) that is different from the definition Eq. (23) of the local volumetric interfacial area used in the two-fluid model based on time-averaging operators. Clearly, the volumetric interfacial areas defined by the Eqs. (3) and (23) *are not the same quantities*. The local volumetric interfacial area (23) is the one appearing in the interfacial transfer terms of the two-fluid model based on time-averaging (Ishii, 1975), and this is the only one that is experimentally measurable.

Finally, the method proposed by Revankar and Ishii (1993) for the measurement of the local volumetric interfacial area, was extended to the measurement of its transport velocity. The four-sensor probe method is theoretically able to handle all two-phase flow regimes, but the accuracy of the measurements decreases with the size of the probe for a given interfacial

configuration. In order to investigate the decrease in the measurement accuracy when the probe size is increased, we have numerically simulated the behavior of such a probe in several artificially generated flows. These flows were bubbly flows with spherical bubbles uniformly distributed in space but other types of flow could be considered. The method used here is extremely fruitful because the values of a_i and $\underline{V}_i$ obtained from probe signals can be compared to their exact values determined from the equations of the interfaces. However, it would be quite difficult to reproduce the interfacial movements in more realistic two-phase flows, because real flows are considerably more complex than those studied here, and in this case the equations of the interfaces are generally unknown.

Nevertheless, the results obtained are quite illuminating and we hope that our approach will be useful for the future experimental studies on interfacial area and its modeling by means of a transport equation.

References

Achard, J.L., 1978. Contribution à l'étude théorique des écoulements diphasiques en régime transitoire. Thèse de doctorat ès sciences, Université Scientifique et Médicale and Institut National Polytechnique de Grenoble.

Aris, R., 1962. Vectors, Tensors and the Basic Equations of Fluid Mechanics. Prentice-Hall, Englewood Cliffs, NJ.

Candel, S.M., Poinsot, T.J., 1990. Flame stretch and the balance equation for the flame area. Combust. Sci. Tech. 70, 1–15.

Coutris, N., 1993. Balance equations for fluid lines, sheets, filaments and membranes. Int. J. Multiphase Flow 19 (4), 611–637.

Delhaye, J.M., 1976. Sur les surfaces volumiques locale et intégrale en écoulement diphasique. C.R. Acad. Sci., Paris, t. 282, Série A, pp. 243–246.

Delhaye, J.M., Achard, J.L., 1977. On the use of averaging operators in two-phase flow modeling. In: Jones, O.C., Bankoff, S.G. (Eds.), Thermal and Hydraulic aspects of Nuclear Reactor Safety, Vol. 1: Light Water Reactors. ASME, New York, pp. 289–332.

Drew, D.A., 1990. Evolution of geometric statistics. SIAM J. Applied Mathematics 50 (3), 649–666.

Garnier, J., 1998. Private communication.

Guido-Lavalle, G., Clausse, A., 1991. Application of the statistical description of two-phase flows to interfacial area assessment. In: VIII ENFIR. Atibaia, SP, 143–146.

Hulburt, H.M., Katz, S., 1964. Some problems in particle technology, a statistical mechanical formulation. Chem. Eng. Science 19, 555–574.

Ishii, M., 1975. Thermo-fluid dynamic theory of two-phase flows. Eyrolles, Paris.

Kataoka, I., Ishii, M., Serizawa, A., 1984. Local formulation of interfacial area concentration and its measurements in two-phase flow. NUREG/CR-4029, ANL 84-68.

Kataoka, I., Ishii, M., Serizawa, A., 1986. Local formulation and measurements of interfacial area concentration. Int. J. Multiphase Flow (12), 505–527.

Kataoka, I., Ishii, M., Serizawa, A., 1994. Sensitivity analysis of bubble size and probe geometry on the measurements of interfacial area concentration in gas–liquid two-phase flow. Nuclear Engineering and Design 146, 53–70.

Kim, S., Fu, X.Y., Wang, X., Ishii, M., 1998. The local interfacial area concentration measurement in a two-phase flow using a four-sensor conductivity probe. ANS Winter Meeting.

Kocamustafaogullari, G., Ishii, M., 1995. Foundation of the interfacial area transport equation and its closure relations. Int. J. Heat Mass Transfer 38 (3), 481–493.

Kojasoy, G., Meinecke, J., Riznic, J., 1998. Interfacial area, velocity and void fraction in two-phase slug flow. In: ICMF'98, Third Int. Conf. on Multiphase Flow, Lyon, France, June 8–12.

Marle, C.M., 1982. On macroscopic equations governing multiphase flows with diffusion and chemical reactions in porous media. Int. J. Eng. Sci. 20 (5), 643–662.

Millies, M., Drew, D.A., Lahey Jr, R.T., 1996. A first order relaxation model for the prediction of the local interfacial area density in two-phase flows. Int. J. Multiphase Flow 22 (6), 1073–1104.

Morel, C., 1997. Modélisation multidimensionnelle des écoulements diphasiques gaz–liquide. Application à la simulation des écoulements à bulles ascendants en conduite verticale. Thèse de doctorat, Ecole Centrale Paris.

Navarro-Valenti, S., Clausse, A., Drew, D.A., Lahey Jr, R.T., 1991. A contribution to the mathematical modeling of bubbly/slug flow regime transition. Chem. Eng. Comm. 102, 69–85.

Revankar, S.T., Ishii, M., 1993. Theory and measurement of local interfacial area using a four-sensor probe in two-phase flow. Int. J. Heat Mass Transfer 36 (12), 2997–3007.

Tien, C.L., Lienhard, J.H., 1979. Statistical Thermodynamics. Hemisphere, Washington, New York, London, pp. 333–370 Revised printing, (chapter 12).